# Applications of quantum dots in optical fiber luminescent oxygen sensors

Pedro A. S. Jorge, Mona Mayeh, Ramazan Benrashid, Paulo Caldas, José L. Santos, and Faramarz Farahi

The potential applications of luminescent semiconductor nanocrystals to optical oxygen sensing are explored. The suitability of quantum dots to provide a reference signal in luminescence-based chemical sensors is addressed. A CdSe–ZnS nanocrystal, with an emission peak at 520 nm, is used to provide a reference signal. Measurements of oxygen concentration, which are based on the dynamic quenching of the luminescence of a ruthenium complex, are performed. Both the dye and the nanocrystal are immobilized in a solgel matrix and are excited by a blue LED. Experimental results show that the ratio between the reference and the sensor signals is highly insensitive to fluctuations of the excitation optical power. The use of CdTe, near-infrared quantum dots with an emission wavelength of 680 nm, in combination with a ruthenium complex to provide a new mechanism for oxygen sensing, is investigated. The possibility of creating oxygen sensitivity in different spectral regions is demonstrated. The results obtained clearly show that this technique can be applied to develop a wavelength division multiplexed system of oxygen sensors.   © 2006 Optical Society of America

*OCIS codes:*   300.0300, 060.2370, 300.6280.

## 1.  Introduction

Oxygen measurement is crucial in many environmental and biomedical applications. Its determination by optical means has many advantages when compared with traditional techniques.[1] In particular, luminescent methods offer high sensitivity, immu-

P. A. S. Jorge, M. Mayeh, R. Benrashid, and F. Farahi are with the Department of Physics and Optical Sciences, University of North Carolina at Charlotte, Charlotte, North Carolina 28223. P. A. S. Jorge (pjorge@inescporto.pt) is also with Unidade de Optoelectrónica e Sistemas Electrónicos, INESC Porto, Rua do Campo Alegre, 687.4169 007 Porto, Portugal, and Departamento de Fisica da Faculdade de Ciências de Universidade do Porto, Rua do Campo Alegre, 687.4169 007 Porto, Portugal. P. Caldas is with Unidade de Optoelectrónica e Sistemas Electrónicos, INESC Porto, Rua do Campo Alegre, 687.4169 007 Porto, Portugal, and the Departamento de Fisica da Faculdade de Ciências da Universidade do Porto, Rua do Campo Alegre, 687.4169 007 Porto, Portugal, and Escola Superior de Tecnologia e Gestão, Institute Politécnico de Viana do Castelo, Av. do Atlântico, Apartado 574, 4901-908 Viana do Castelo, Portugal. J. L. Santos is with Unidade de Optoelectrónica e Sistemas Electrónicos, INESC Porto, Rua do Campo Alegre, 687.4169 007 Porto, Portugal, and the Departamento de Fisica da Faculdade de Ciências da Universidade do Porto, Rua do Campo Alegre, 687.4169 007 Porto, Portugal.

nity to electromagnetic interference, no oxygen consumption, and fast response times. Additionally, the association of luminescence spectroscopy techniques with optical fibers provides new possibilities such as miniaturization and remote sensing.[2–5] The dynamic quenching of luminescence by oxygen is the most widely used sensing mechanism for the optical detection of this gas. Ruthenium complexes are among the most popular oxygen sensing dyes.[6] When excited by a blue LED they emit a very bright luminescent signal that is strongly quenched by oxygen. In addition, their relatively long lifetimes are suitable for frequency domain techniques to be used as a detection mechanism.[7,8] Their immobilization in solgel and polymer matrices is straightforward, making them suitable for integrated optics and optical fiber sensor applications.[9,10]

Both the luminescence intensity, $I$, and the excited state lifetime, $\tau$, of the sensing dye are quenched by oxygen. This mechanism is described by the Stern–Volmer equation[11]

$$\frac{I_0}{I} = \frac{\tau_0}{\tau} = 1 + K_{SV}[O_2], \qquad (1)$$

where $I_0$ and $\tau_0$ are the unquenched luminescence intensity and lifetime, respectively, $K_{SV}$ is the Stern–

Volmer constant, and $[O_2]$ is the concentration of oxygen. This equation shows that measurement of either the intensity or the lifetime of the luminescent signal can provide information about oxygen concentration. However, the direct measurement of these parameters has associated problems. Intensity based sensors should have a reference signal in order to avoid interference due to optical power fluctuations caused by optical source drift, coupling efficiency variations, etc. Conversely, direct measurement of the lifetime demands high-speed electronics and fast pulsed optical sources. Frequency domain techniques can be used to avoid these problems. If the optical source is sinusoidally modulated, the luminescent emission would also vary sinusoidally but present a phase shift, relative to the modulation signal, that is proportional to the lifetime and thus to the oxygen concentration. This is already an established technology; however, some limitations exist that leave room for improvement. Leaching and photobleaching of the sensing dye usually degrade sensor performance. Moreover, it has been reported that photobleaching of the dye also changes the excited state lifetime and the phase response.[12] Additionally, an intensity based system is often a simpler, less expensive alternative. Most common intensity reference schemes include the use of a second analyte-insensitive dye and ratiometric detection of two wavelengths.[13] Ratiometric schemes can also be used with detection of backreflected excitation radiation (corresponding to Fresnel reflections in the fiber system). However, most dyes available suffer from photobleaching and full reference cannot be achieved with the ratio of luminescence to the excitation radiation.

Another critical problem, especially in environmental applications, where the determination of the analyte in multiple points is needed, is the lack of a multiplexing approach for optical oxygen sensing. Currently the available technologies are usually developed for single point measurements. Simultaneous measurement of several parameters requires a multiplexing sensing system. At present a few functional luminescence-based sensing systems do this. They rely on several optical fibers, each leading to a measurement point for a specific parameter.[14] Also, the possibility of distributed chemical sensing with luminescent cladding optical fibers has been addressed, but no further progress has been reported.[15] It would be more desirable to incorporate multiple luminescent sensors in a fiber-optic-distributed sensor network.

Recent developments in nanomaterials have provided new possibilities in the area of chemical and biological sensors. Luminescent semiconductor nanocrystals, or quantum dots (QDs), are especially attractive in this area, and have great potential to solve some of the problems associated with luminescent sensors. QDs are nanometer scale particles of semiconductor material (e.g., CdSe or CdS).[16] Due to their small size they are subjected to the quantum confinement effect, meaning that the electronic energy distribution of these particles will be determined by their physical size. This provides them with unique optical properties that are highly favorable when compared to traditional fluorophores, and can be used to great advantage in a large number of bioassays and chemical sensing techniques.[17–19] In contrast with traditional dyes, which have broad emission spectra with a characteristic to have a long red tail, nanocrystal QDs present a very symmetrical (Gaussian) and relatively narrow emission spectrum. Additionally, similar to bulk semiconductor materials, nanocrystal QDs will absorb any wavelength to the blue of the emission peak, i.e., any photon with energy higher than that of the bandgap will be absorbed. They present high quantum yields and an outstanding photostability. The ability to tune their optical properties can be achieved by simply changing the nanoparticle size or the semiconductor material. At present, they are available in a variety of emission wavelengths (from 350 to 2000 nm), and can be provided in the form of colloidal suspensions suitable to be immobilized in polymers or solgel based materials. This combination of properties gives QDs great versatility.

In this paper we propose to explore the potential applications of semiconductor nanocrystals for luminescent oxygen sensors. Due to their high resistance to photobleaching QDs can provide a very stable reference signal. In this work we use CdSe nanoparticles, in combination with a ruthenium complex, to obtain a self-referenced, intensity-based, luminescent oxygen sensor. The possibility of changing the spectral signature of a luminescent oxygen sensor is also investigated. For this purpose, CdTe nanoparticles are combined with a ruthenium complex to enhance the oxygen sensitivity in the infrared. Results are obtained that indicate the possibility of wavelength multiplexing of oxygen sensors using QDs.

## 2. Experimental Details

### A. Preparation of Samples

Different core-shell semiconductor nanocrystals were acquired from Nanoco (CdSe–ZnS with an emission peak at 520 nm, $QD_{520}$) and Evident Technologies (CdTe–ZnS with an emission peak at 680 nm, $QD_{680}$). Core-shell QDs were chosen because they have a semiconductor material core (e.g., CdSe), coated with a passivating layer of ZnS, which ensures a higher stability of their luminescent properties and some immunity to oxidation and other impurities. The nanocrystals were used to dope different solutions of a nonhydrolytic solgel[20] with a concentration of 5 mg/ml. After stirring for 6–8 h, to obtain a homogeneous mixture, the solutions were filtered through a 0.1 μm filter. Thin films and bulk samples with different characteristics were made by spin coating (1500 rpm) or molding in silicone. All the samples were subject to thermal annealing under a nitrogen flux. The exact baking times and temperatures (ranging from 100 °C to 200 °C) depended on the sample thickness. After thermal treatment, a dense glass material was formed that provided the QDs further protection from oxidation.
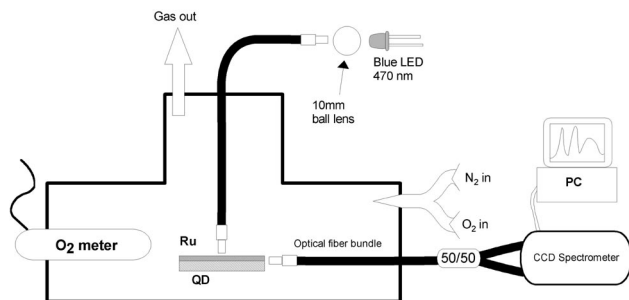
Fig. 1. Experimental setup used to test CdSe QDs as an intensity reference in a luminescent oxygen sensor.

Two different ruthenium complexes were used as oxygen sensors in the experiments: [Ru(bpy)$_3$]-Tris(2,2′-bipyridine) ruthenium (II) chloride hexahydrate and [Ru(dpp)]-Tris(4,7-diphenyl-1,10-phenanthrolin) (I) chloride hexahydrate. Both dyes have strong luminescent emissions at 620 nm when excited with blue radiation (470 nm). The intensity and the excited state lifetime of their luminescence are both highly quenched in the presence of oxygen. The lifetimes of Ru(bpy) and Ru(dpp) are approximately 1 and 5 μs, respectively. The latter has increased sensitivity to oxygen.

Different samples of thin films and bulk glasses, doped with the sensing dyes, were produced by using distinct solgel protocols. The same process that was used to encapsulate the QDs in a nonhydrolytic solgel was used to produce thin films and bulk glass samples doped with Ru(bpy) and Ru(dpp). However, the samples produced in this way had low oxygen sensitivity due to the low porosity of the resulting solgel material. This way a hydrolytic solgel was also used to produce more sensitive samples.[21] Methyltriethoxysilane (0.252 mol), dimethyldimethoxysilane (0.252 mol), and water (0.389 mol) were mixed for 1 h at room temperature. Dibutoxy aluminoxy triethoxy silane (0.107 mol) was then added and mixing was continued under nitrogen and at room temperature for 20 h. Ru(bpy) was then used to dope different solgel solutions with concentrations of 15 and 10 mM. The solutions obtained were filtered through a 0.1 μm filter and different films were then produced by spin coating (1500 rpm). The films were cured at 100 °C for 2 h and at 120 °C for 6 h. Thin films with a thickness of approximately 7.5 μm were obtained.

### B. Quantum Dots as Intensity References

To test the possibility of using QD luminescence as a reference signal in an optical oxygen sensor the experimental setup displayed in Fig. 1 was implemented. A hydrolytic solgel thin film doped with Ru(bpy) (10 mM) was used as the sensing element. The reference was provided by a bulk glass sample (approximately 1 mm thick) doped with QD$_{520}$. Both samples were placed in close contact inside a sealed chamber with two valves to supply nitrogen and oxygen as needed. The flux of each gas was controlled to adjust the level of O$_2$ inside the chamber. A conven-

tional oxygen meter was also used to monitor the oxygen concentration. A blue LED (470 nm, Nichia) was used as the excitation optical source. The LED radiation was guided to the samples by a 4 mm diameter optical fiber bundle. Both luminescent signals were detected by using a 4 mm diameter $Y$ splitter optical fiber bundle, which guided the sensor output into the two channels of an S2000 Ocean Optics miniature spectrometer (channel 1 ranging from 282 to 607 nm, with no filter, and channel 2 ranging from 575 to 835 nm, with a built-in long-pass filter with a cutoff wavelength at 550 nm). The detection fiber was oriented at 90° to the excitation fiber to avoid excessive optical background noise from the backreflected excitation radiation.

Some precautions were taken to ensure that the QD luminescence was independent of the oxygen level in the chamber. The nonhydrolytic solgel was cured at an elevated temperature to reduce the porosity of the resulting glass and minimize the permeability to oxygen. Additionally, using QDs with a core-shell structure provided further protection of the luminescent core from oxidation and other possible contaminations. Finally, QD$_{520}$ was used to avoid spectral overlap with either the excitation source or the sensing dye. Only wavelengths lower than 520 nm are absorbed by these QDs, therefore its luminescent intensity will be affected by the excitation radiation but not by the Ru(bpy) emission. Because of these considerations oxygen had no effect on the QD's emission, which was proportional only on the exciting optical power. In this situation the ratio between the emission of the Ru(bpy), which depends on oxygen concentration and on the excitation optical power level, with the emission of QD$_{520}$, should be independent of any optical power drift in the sensing system. Some tests were performed to assess the efficiency of this scheme.

### C. Quantum Dots as Oxygen Sensors

Core-shell CdTe QDs, with an emission at 680 nm, were used to provide a luminescent oxygen sensor with a different spectral profile. Because these QDs have a protective shell and were immobilized in a dense glass material, they did not suffer from direct oxidation. In spite of this, because their emission peak is at 680 nm, these particular QDs can absorb the luminescent emission of the ruthenium complexes, hence becoming sensitive to the oxygen concentration. However, the LED excitation radiation can also be absorbed by the nanocrystals. This way two contributions for the QD luminescence can coexist: an oxygen sensitive signal due to excitation by the sensing dye emission and a signal with no sensitivity to oxygen due to direct excitation by the LED. The ideal situation would be to ensure that only the former is present.

To test this idea different sensing configurations were used. A bulk glass sample (thickness of approximately 1 mm) doped with QD$_{680}$ was combined with different oxygen-sensitive samples (doped with the ruthenium dyes) and was tested in the setup of Fig. 2.
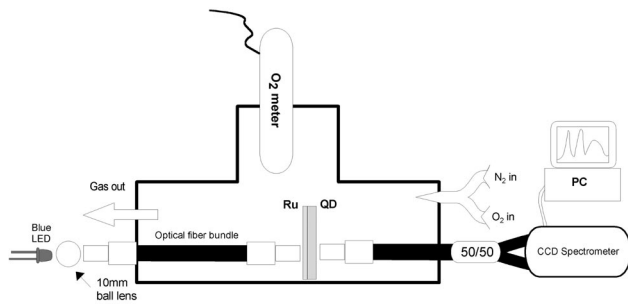
Fig. 2. Experimental setup used to test the sensitivity of different QDs and sensing dye combinations.



Fig. 3. Spectral behavior of the LED, the reference signal (QD), and the sensing dye (Ru) when (a) $P_{LED}$ was decreased from 100% to 82% and 63% in a 21% $O_2$ atmosphere and (b) the $O_2$ level was set to 0%, 20%, and 100%, with constant $P_{LED}$.

The same excitation source and detection instrumentation that were used in the setup of Fig. 1 were also used in this setup. However, as shown in Fig. 2, in this experiment a transmission configuration was used instead. In all the tests performed the sample doped with sensing dye was placed facing the incoming LED radiation; the QD$_{680}$ bulk glass was then placed in close contact with the sensing sample. In some of the tests a long-pass filter (with a cutoff at 600 nm) was placed between the sensing sample and the QD$_{680}$ sample. This way, direct excitation of the QDs by the excitation radiation could be eliminated.

Different test samples were evaluated by submitting the sensors to saturated atmospheres of oxygen and nitrogen. A spectral quenching coefficient, $\alpha(\lambda)$, was defined to compare the sensitivity of sensors,

$$\alpha(\lambda) = \frac{P_{O_2}(\lambda)}{P_{N_2}(\lambda)}, \qquad (2)$$

where $P_{O_2}(\lambda)$ and $P_{N_2}(\lambda)$ are the optical powers of the luminescent emission at each wavelength in saturated atmospheres of $O_2$ and $N_2$, respectively. The parameter $\alpha$ is a measure of oxygen sensitivity at each wavelength. The usual quenching efficiency, $Q$, defined by

$$Q = \frac{I_{N_2} - I_{O_2}}{I_{N_2}}, \qquad (3)$$

was also evaluated. In this equation $I_{N_2}$ and $I_{O_2}$ are the luminescence intensities in $N_2$ and $O_2$ saturated atmospheres, respectively.

## 3. Results and Discussion

### A. Quantum Dots as Intensity References

Two simple experiments were carried out to demonstrate the proposed intensity reference scheme by using the experimental setup shown in Fig. 1. First, the excitation optical output power of the LED, $P_{LED}$, was successively set at three different levels: 100%, 82%, and 63%. This was achieved by changing the LED's drive current. During this test the concentration of oxygen remained constant (21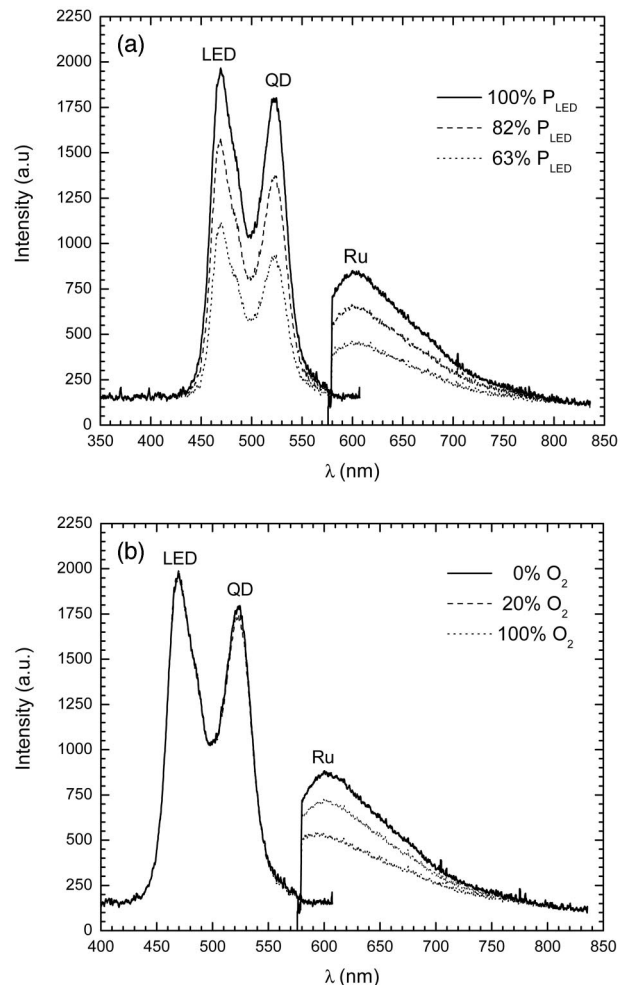%). In the second test, the oxygen level of the chamber was changed in a controlled way while the drive current of the LED was set to a constant value. The experimental results obtained with these tests can be observed in Figs. 3(a) and 3(b), respectively. As expected, when the LED output power was decreased, the luminescent emissions of the sensing dye and of the QDs were decreased in the same proportion. However, when the oxygen level was successively set to 0%, 20%, and 100%, only the emission of the sensing dye responded to the changes in concentration. The luminescent intensity of the QDs remained constant and proportional to the LED output.

Some overlap was observed between the emission of the LED and that of the QDs, but the spectral peaks of the optical source, the reference signal, and the sensor were easily discriminated by the CCD spectrometer. With adequate software it was straightforward to acquire electrical signals proportional to the optical power of the LED, QD, and Ru(bpy). The results shown in Figs. 3(a) and 3(b) indicate that performing a ratio operation between the signal of the sensing dye, $P_{Ru}$, and the signal of the nanocrystal, $P_{QD}$, will yield a
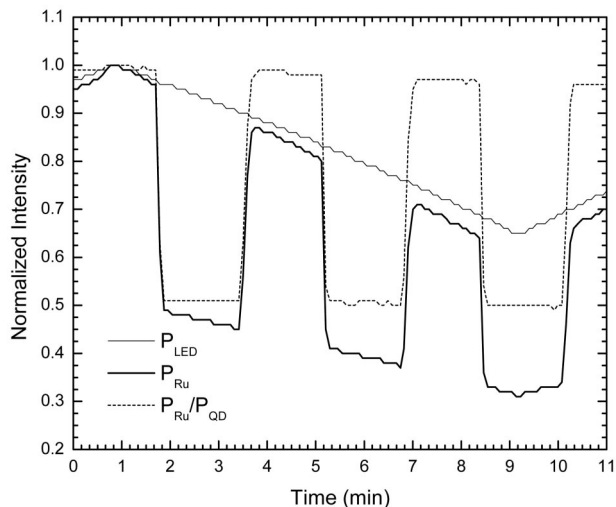
Fig. 4. Sensor response ($P_{Ru}$ and $P_{Ru}/P_{QD}$) to $O_2/N_2$ saturation cycles while $P_{LED}$ changed slowly from 100% to 70%.



Fig. 5. Response of $P_{Ru}$ and $(P_{Ru} - P_{QD})/(P_{Ru} + P_{QD})$ to changes in LED optical power.

normalized output that is independent of the level of excitation optical power in the sensing system. In addition, $P_{Ru}/P_{QD}$ will be proportional to the concentration of $O_2$ in the test chamber. To verify the degree of immunity to fluctuations of the excitation optical power obtained with this scheme, the solgel samples were submitted to saturation cycles of $O_2/N_2$, while the drive current of the LED was modulated by a slowly varying triangular wave that changed the LED output from 100% to 70%. To improve the signal-to-noise ratio the dark spectrum of the CCD was subtracted from the acquired data before the ratio operation was performed. The results obtained in this test can be observed in the plot of Fig. 4.

It is clearly shown in Fig. 4 that, while the luminescence output of Ru(bpy) was strongly affected by the oxygen level in the chamber and by changes in excitation optical power, the intensity ratio, $P_{Ru}/P_{QD}$, only responded to variations of $O_2$ concentration. Further tests demonstrated that a decrease of 82% in $P_{Ru}$ caused by a decrease in the excitation optical power affected our measured oxygen concentration by only 4%. The immunity was further improved when the outputs of the sensing dye and the QDs' reference were normalized according to the operation $(P_{Ru} - P_{QD})/(P_{Ru} + P_{QD})$. In this case the error was reduced to 2.7% after a near 80% decrease in the LED optical power. In this particular configuration, the slight overlap between the spectrums of LED and the QDs prevented further improvement. Then a smaller detection fiber (400 μm diameter) was used and it was positioned such that no LED radiation could be collected. In this case the highest variation observed was smaller than 1.5%, which was within the noise level of our system (Fig. 5). This figure clearly shows that, regardless of the intensity fluctuation of the excitation source, the sensor response is directly proportional to the oxygen concentration. The same result can be obtained with more selective filtering or by using a QD with a longer wavelength
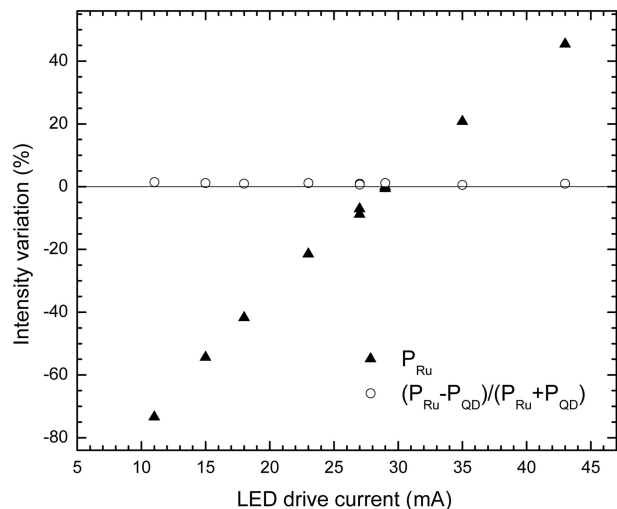
and no overlap with the excitation source spectrum. These results clearly establish semiconductor nanocrystals as suitable intensity references in luminescence-based optical sensors.

While this scheme compensates for any optical power fluctuation or loss within the sensing system, it does not solve the problem of photobleaching of the sensing dye. To assess the effect of this problem in our system, the degree of photobleaching was evaluated in three different samples: a hydrolytic solgel thin film (thickness of 7.5 μm) doped with Ru(bpy) (15 mM), a hydrolytic solgel thin film (7.5 μm) doped with Ru(bpy) (10 mM), and a nonhydrolytic solgel thin film doped with Ru(bpy) (10 mM) with a thickness of approximately 5 μm. All the samples were irradiated with approximately 20 mW/cm² (using the blue LED), for periods ranging from 10 to 24 h. The results obtained can be observed in Fig. 6.

The hydrolytic solgel samples showed a high degree of photodegradation. The maximum effect was observed for the sample doped with 15 mM where, after 10 h of irradiation, the luminescent intensity decreased by approximately 30%. For the sample with 10 mM, the decrease was 18% after 10 h and 27% after 17 h. On the other hand, the nonhydrolitic sample showed no sign of photodegradation after 23 h of continuous irradiation. Under the same conditions, a 1 mm thick sample, doped with $QD_{520}$ and exposed for 16 h, presented a constant luminescent output demonstrating a very high photostability.

This means that a combination of $QD_{520}$ with Ru(bpy), both immobilized in nonhydrolytic solgel, would make a very stable self-referenced oxygen sensor, suitable for long term use. The photostability of the Ru(bpy) when immobilized in nonhydrolitic solgel, however, results from the low permeability to oxygen of this material. This way the quenching efficiency, $Q$, of such a sensor would be very small when compared with the values that can be obtained with porous solgel samples. The quenching efficiency of
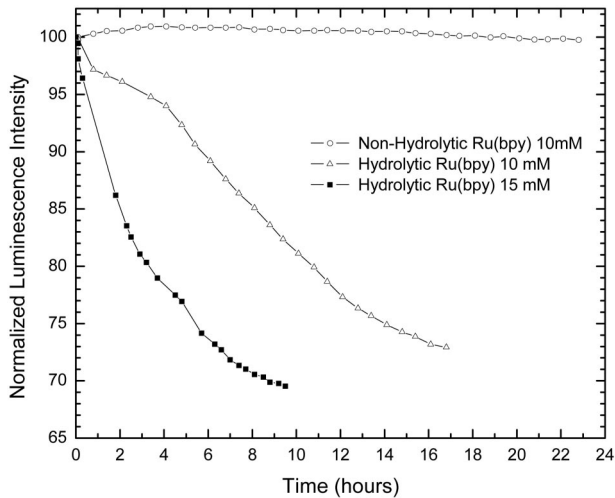
Fig. 6. Time behavior of the luminescent output of different solgel films doped with Ru(bpy) while the samples are irradiated with blue radiation (20 mW/cm$^2$).

the three samples tested was measured. While with both hydrolytic samples a quenching efficiency of approximately 55% was estimated, with the nonhydrolytic samples values of approximately 20% were obtained. Taking into account that, with other solgel protocols, values of $Q$ as high as 95% can be obtained, this is a low sensitivity. However, for long-term applications where stability is more important than sensitivity, such as for some environmental applications, the results obtained can provide an interesting solution.

### B. Quantum Dots as Oxygen Sensors

In the first experiment a bulk glass sample doped with QD$_{680}$ was combined with a thin film of hydrolytic solgel doped with Ru(bpy) (10 mM) as shown in Fig. 2. In this situation, the amount of excitation optical power crossing the sensing film without being absorbed and reaching the QDs was very high. This way the QDs' emission was mainly due to this direct excitation and no response to oxygen was observed. Changing the thin film by a bulk glass sample (approximately 1 mm thick) of nonhydrolytic solgel doped with Ru(bpy) (10 mM) resulted in an almost complete absorption of the LED radiation by the sensing sample. In this situation, the QDs' emission was mainly due to the absorption of the Ru(bpy) radiation and therefore dependency on the oxygen concentration could be observed. However, due to the increased thickness of the sensing sample and because Ru(bpy) was immobilized in a dense glass material, the quenching efficiency of this configuration was small ($Q \approx 10\%$).

To obtain a higher quenching efficiency the oxygen-sensitive dye was changed to Ru(dpp). A thin film of nonhydrolitic solgel doped with this dye (approximate thickness of 50 μm) was tested for three different cases where the sensing element was (1) a single Ru(dpp) film, (2) a Ru(dpp) film followed by the QD$_{680}$ layer, and (3) a Ru(dpp) film followed by a long-pass
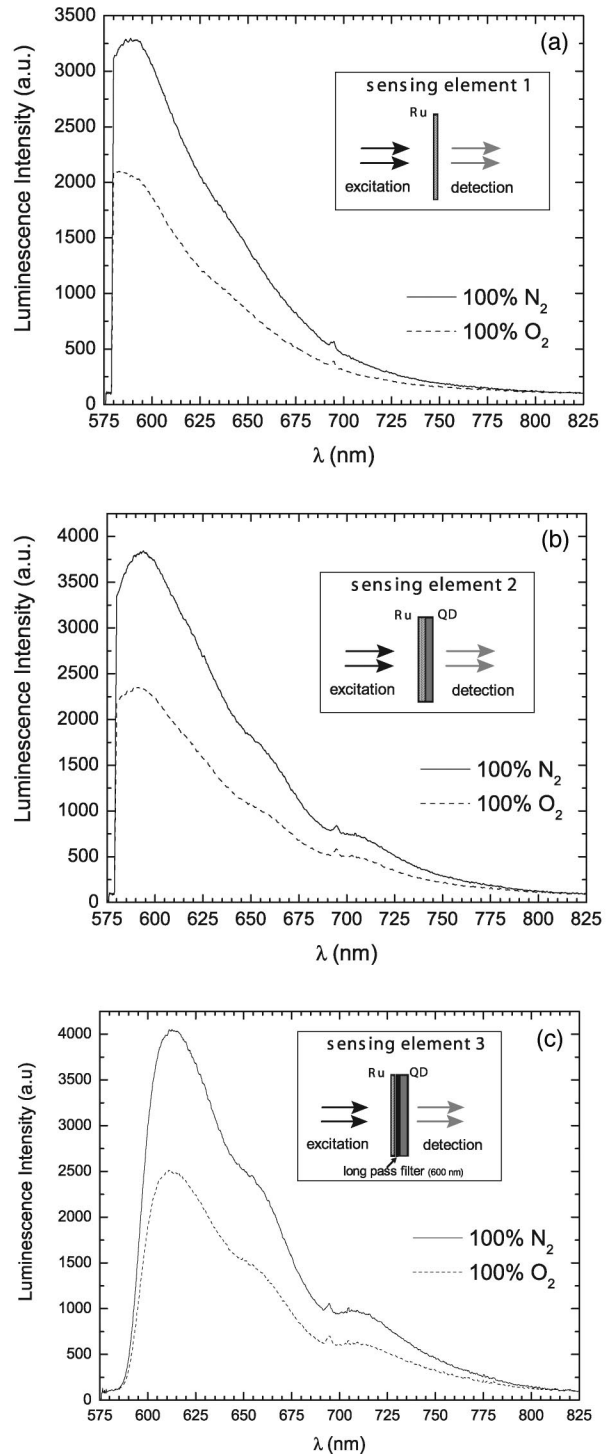


Fig. 7. Spectral responses in saturated atmospheres of N$_2$ and O$_2$. Insets, a scheme of the sensing configuration: (a) Ru(dpp); (b) Ru(dpp) + QD$_{680}$; (c) Ru(dpp) + long-pass filter (600 nm) + QD$_{680}$.

filter (cutoff at 600 nm) and the QD$_{680}$ sample. These sensor configurations are depicted in the insets of Figs. 7(a)–7(c), respectively. Configuration (3) was used to assess the influence of direct excitation of the QDs from the LED.

The spectral response obtained in saturated atmospheres of N$_2$ and O$_2$ for each configuration can be
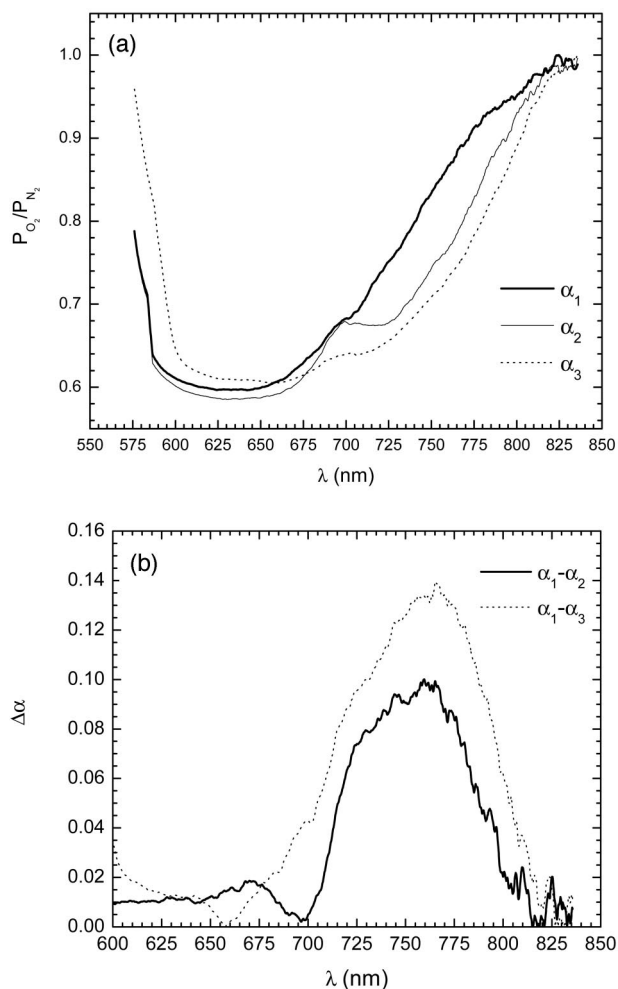
Fig. 8. (a) Oxygen sensitivity, $\alpha(\lambda)$, for configurations 1–3; (b) sensitivity enhancement of configurations (2) and (3) relative to configuration (1).

observed in Figs. 7(a)–7(c). Figure 7(a) shows the typical response of Ru(dpp) in the presence of oxygen. A quenching efficiency of 35.8% was measured. This relatively small change is a consequence of using a very dense nonhydrolytic solgel glass. Similar results were obtained with the other two sensor configurations. In those two cases the emission peak of the QDs at approximately 710 nm could be observed. Careful analysis of the experimental results revealed that, when compared with configuration (1), configurations (2) and (3) show enhanced oxygen sensitivity in the spectral region of 700–800 nm (which corresponds to the QDs' emission). This increase in sensitivity can be quantified by plotting coefficient $\alpha$ as a function of wavelength. In Fig. 8(a) the plots of $\alpha_1$, $\alpha_2$, and $\alpha_3$, corresponding, respectively, to configurations (1), (2), and (3), can be observed. Figure 8(b) shows the differences in sensitivity $\alpha_1$-$\alpha_2$ and $\alpha_1$-$\alpha_3$. It can be clearly observed that, configurations (2) and (3) present increased oxygen sensitivity in the spectral region corresponding to the QDs' emission. The enhancement is higher in configuration (3), where the filter was used, indicating that in configuration (2)

some of the LED radiation was reaching the QDs. For the implementation of a practical system careful design of the sensing head is needed to avoid this problem.

It can be seen from Fig. 8(b) that the improvement in quenching coefficient $\alpha$ is maximum at approximately 760 nm. At this particular wavelength, information derived from this figure indicates that the sensor design shown in configuration (2) is more sensitive than in configuration (1) by a factor of 1.7, while configuration (3) shows a twofold increase.

These results demonstrate that it is possible to obtain oxygen sensitivity in different spectral regions. The ideal situation would be to have near-infrared QDs with no spectral overlap with the ruthenium emission. The application of this principle with QDs of different emission peaks combined with the sensing dye would allow us to obtain a set of oxygen sensors with different spectral signatures suitable for wavelength multiplexing.

At the time when these experiments were conducted the CdTe QDs emitting at 680 nm were the only near-infrared core-shell QDs available. Some PbSe QDs with higher emission wavelengths (1300–1500 nm) were tested. However, these were not core-shell QDs, and without the protection of the passivating layer their luminescence was strongly quenched upon solgel immobilization. Nevertheless, QD technology is rapidly evolving and core-shell QDs with IR emission will soon be available, providing interesting solutions for near-infrared wavelength multiplexed chemical sensors. QDs with higher emission wavelengths will also enhance the performance of sensors based on configurations (2) and (3) since their emission spectra will not overlap with that of the sensing dye.

## C. Temperature Behavior of Quantum Dots

The behavior of the luminescent properties of QDs with temperature has recently been reported to have suitable characteristics for application as temperature probes.[22] Temperature changes the intensity, the peak wavelength, and the spectral width of the QDs' luminescent emission in a linear and reversible way. Although it seems that the temperature dependency of QDs can be a problem for the applications that we proposed in this paper, this can in fact offer an added advantage. The response of luminescence-based chemical sensors, such as optical oxygen sensors, is always temperature dependent. For univocally determining the chemical parameter, the simultaneous determination of temperature must be performed.

We have recently demonstrated that QD luminescence can be used to provide a self-referenced, intensity based, temperature measurement.[23] The temperature information is obtained by measurement of the shift in the peak wavelength. The luminescent intensity of the QDs also changes in a linear fashion with temperature. This way, the temperature information obtained from the shift in the peak wavelength can be used to correct for the intensity variations induced by temperature. In this context, QDs can still be used either as a reference

signal or as an oxygen sensor while simultaneously providing information about temperature.

## 4. Conclusion

The potential applications of QDs to optical oxygen sensing were explored. The use of semiconductor nanocrystals to provide a reference signal in a fiber-optic oxygen sensor was demonstrated. The experimental results clearly show that an oxygen sensor based on the quenching of luminescence of Ru(bpy) could be designed that is independent of fluctuations in the excitation optical power.

The possibility of obtaining an oxygen sensor with a different spectral signature by combining a ruthenium complex with semiconductor nanocrystals was also demonstrated. The use of different QDs in the infrared region will allow the implementation of wavelength multiplexed oxygen sensors with the potential for application in sensing networks for environmental monitoring.

Since QD luminescence is temperature dependent, incorporation of QDs in an oxygen sensor would enable simultaneous measurement of temperature and oxygen concentration to be made. Since the spectral properties of QDs could be tailored by selecting their composition and controlling the size of nanoparticles these schemes might be extended to other luminescence-based chemical sensors, making QDs a useful tool in this field.

## References

1. C. D. Johnson and D. W. Paul, "*In situ* calibrated oxygen electrode," Sens. Actuators B **105,** 322–328 (2005).
2. O. S. Wolfbeis, "Fiber optic chemical sensors and biosensors," Anal. Chem **72,** 81R–89R (2002).
3. G. Holst and B. Mizaikoff, "Fiber optic sensors for environmental applications," in *Handbook of Optical Fiber Sensing Technology,* J. M. Lopez-Higuera, ed. (Wiley, 2002), pp. 729–755.
4. M. K. Krihak and M. R. Shahariari, "Highly sensitive, all solid state fibre optic oxygen sensor based on the sol-gel coating technique," Electron. Lett. **32,** 240–242 (1996).
5. I. Klimant, F. Ruckruh, G. Liebsch, A. Stangelmayer, and O. S. Wolfbeis, "Fast response oxygen micro-optodes based on novel soluble ormosil glasses," Mikrochim. Acta **131,** 35–46 (1999).
6. E. R. Carraway, J. N. Demas, B. A. DeGraff, and J. R. Bacon, "Photophysics and photochemistry of oxygen sensors based on luminescent transition-metal complexes," Anal. Chem. **63,** 337–342 (1991).
7. M. T. Murtagh, D. E. Ackley, and M. R. Shahriari, "Development of a highly sensitive fibre optic $O_2$/DO sensor based on a phase modulation technique," Electron. Lett. **32,** 477–479 (1996).
8. C. McDonagh, C. Kolle, A. K. McEvoy, D. L. Dowling, A. A. Cafolla, S. J. Cullen, and B. D. MacCraith, "Phase fluorometric dissolved oxygen sensor," Sens. Actuators B **74,** 124–130 (2001).
9. C. M. McDonagh, P. Bowe, K. Mongey, and B. D. MacCraith, "Characterisation of porosity and sensor response times of sol-gel-derived thin films for oxygen sensor applications," J. Non-Cryst. Solids **306,** 138–148 (2002).
10. I. Klimant and O. S. Wolfbeis, "Oxygen-sensitive luminescent materials basead on silicone-soluble ruthenium diimine complexes," Anal. Chem. **67,** 3160–3166 (1995).
11. J. R. Lakowicz, *Principles of Fluorescence Spectroscopy,* 2nd ed. (Kluwer-Plenum, 1999).
12. P. Hartmann, M. J. P. Leiner, and P. Kohlbacher, "Photo-bleaching of a ruthenium complex in polymers used for oxygen optodes and its inhibition by singlet oxygen quenchers," Sens. Actuators B **51,** 196–202 (1998).
13. A. Song, S. Parus, and R. Kopelman, "High-performance fiber-optic pH microsensors for practical physiological measurements using a dual-emission sensitive dye," Anal. Chem. **69,** 863–867 (1997).
14. G. Holst, R. N. Glud, M. Kuhl, and I. Klimant, "A microoptode array for fine-scale measurement of oxygen distribution," Sens. Actuators B **38,** 122–129 (1997).
15. R. A. Lieberman, L. L. Blyler, and L. G. Cohen, "A distributed fiber optic sensor based on cladding fluorescence," J. Lightwave Technol. **8,** 212–220 (1990).
16. V. I. Klimov, "Nanocrystal quantum dots," Los Alamos Sci. **28,** 214–220 (2003).
17. C. J. Murphy, "Optical sensing with quantum dots," Anal. Chem. **74,** 520A–526A (2002).
18. J. K. Jaiswal and S. M. Simon, "Potentials and pitfalls of fluorescent quantum dots for biological imaging," Trends Cell Biol. **14,** 497–504 (2004).
19. A. J. Sutherland, "Quantum dots as luminescent probes in biological systems," Curr. Opin. Solid State Mater. Sci. **6,** 365–370 (2002).
20. R. Benrashid and P. Velasco, "High performance sol-gel spin-on glass materials," U.S. patent 0022697 A1 (3 February 2005).
21. C. M. McDonagh, B. D. MacCraith, and A. K. McEvoy, "Tailoring of sol-gel films for optical sensing of oxygen in gas and aqueous phase," Anal. Chem. **70,** 45–50 (1998).
22. G. W. Walker, V. C. Sundar, C. M. Rudzinski, A. W. Wun, M. G. Bawendi, and D. G. Nocera, "Quantum-dot optical temperature probes," Appl. Phys. Lett. **83,** 3555–3557 (2003).
23. P. A. S. Jorge, M. Mayeh, R. Benrashid, P. Caldas, J. L. Santos, and F. Farahi, "Self-referenced intensity based optical fiber temperature probes for luminescent chemical sensors using quantum dots," in *17th International Conference on Optical Fibre Sensors,* M. Voet, R. Willsch, W. Ecke, J. Jones, and B. Culshaw, eds., Proc. SPIE **5855,** 42–45 (2005).